# Charge Transfer of Rydberg H Atoms at a Metal Surface

E. So, M. Dethlefsen, M. Ford, and T. P. Softley

*Department of Chemistry, University of Oxford, Chemistry Research Laboratory, Oxford OX1 3TA, United Kingdom*

(Received 21 April 2011; published 22 August 2011)

The charge transfer of Rydberg hydrogen atoms at a metal surface is investigated for the first time. The surface ionization of Stark states with various electron density distributions with respect to the surface is examined. Unlike the nonhydrogenic species studied previously, genuine control over the orientation of the electronic wave function in the surface-ionization process is demonstrated. A comparison of the results for a range of collisional velocities for the most redshifted Stark state with principal quantum numbers $n = 20$–$36$ with the classical over-the-barrier approach shows a good agreement for the onset of the ion signal, but the shallow rise in signal is not accounted for. An excellent fit of the experimental results can be achieved using a simple semiempirical model.

DOI: 10.1103/PhysRevLett.107.093201 PACS numbers: 34.35.+a, 34.50.Fa, 34.70.+e

The interaction of atoms, molecules or ions in the gas phase with a metallic surface commonly involves the transfer of electrons. Such processes are of fundamental importance in surface physics and chemistry, catalysis, vapor deposition, and in techniques such as field-ionization microscopy. Charge transfer from electronically excited ''Rydberg'' species to surfaces is important in plasmas [1], ion-sputtering [2], and for some atom-chip experiments [3,4], and has been proposed as a route to controlled deposition [5]. The Rydberg electron binding energy is small and charge transfer to many metals takes place via resonant interaction with the unoccupied conduction band. The atom-surface separation at which the charge transfer occurs depends on both the properties of the Rydberg state and of the metal surface. Classical theory [6] predicts an $n^2$ scaling (where $n$ is the Rydberg electron principal quantum number) of the surface-ionization distance, reflecting the mean orbital radius ($\langle r \rangle \propto n^2$), and this has been confirmed in previous experiments [7–9]. In a homogeneous electric field, the levels of a given $n$ are split into a manifold of Stark states described by a parabolic quantum number $k$. The electron density distribution in these states may be highly asymmetric, especially for the extreme members of the Stark manifold. Stark states can be spectroscopically selected with their electron density directed either towards the surface or towards the vacuum or with more complex nodal patterns. Intuitively it would be expected that the surface-oriented Stark states would ionize further from the surface compared to vacuum-oriented states, and calculations carried out for H atoms [10–12] appear to confirm this. However, experiments involving nonhydrogenic species [13,14], have shown that the ionization distances show little or no dependence on the $k$ quantum number of the initially populated Stark state, attributable to the ''scrambling'' of polarization on passage through numerous avoided energy level crossings as the surface is approached [13,15].

Theoretical studies of Rydberg-surface interactions, including classical [6] and semiclassical approaches [16], perturbation theory [17], scattering theory [18], complex scaling [10], and quantum wave packet propagation [12,15] have focused mainly on the H atom surface system as this is the most tractable one and has additional intrinsic symmetry [19]. To date, however, only experiments involving alkali metal [7], xenon [8,20] and $H_2$ molecules [9,14] have been carried out. In this work we carry out the first experimental study of the interaction of Rydberg H atoms with a metal surface, providing an opportunity for genuine comparison of theory with experiments. We demonstrate experimentally the fundamental difference between the excited-H atom behavior and that of other atomic or molecular systems: the Rydberg charge transfer shows a strong dependence on the $k$-quantum number showing that the electron polarization is not scrambled on approach to the surface, allowing a new level of control of the surface-atom interaction.

In the experimental setup, H atoms are created by photodissociation of $NH_3$ in a supersonic beam. A 193 nm ArF excimer laser (10 Hz, 7.5 mJ) is weakly focused into a quartz capillary tube mounted on the end of the pulsed nozzle [21]. For a helium seeded beam ($He:NH_3$, 20:1, 2 bar backing pressure), the H atoms equilibrate with the velocity of the He carrier gas within the quartz capillary and the mean velocity is $\sim 1600$ ms$^{-1}$. ''Fast'' (unseeded) H atoms are produced by photodissociation in pure $NH_3$ (700 mbar backing pressure); these atoms escape the $NH_3$ carrier gas and travel at a mean velocity of $\sim 2500$ ms$^{-1}$. After expansion at the end of the capillary, the atomic beam passes through a 1 mm diameter skimmer and travels 46 cm to the interaction region of the UHV chamber. The H atoms are directed towards an evaporated gold surface with an rms flatness of $\sim 1$ nm [9] mounted on a vacuum manipulator. For the work presented here, the grazing incidence angle is held at a constant 15°.

 © 2011 American Physical Society

The H atoms are excited ~2 mm from the surface to selected high-$n$ levels ($n = 20$–$40$) with two counterpropagating laser beams using a two-color resonant excitation scheme via the $2p$ level as an intermediate. The vacuum ultraviolet (VUV) beam at 121.6 nm is produced by frequency tripling of a frequency-doubled Nd:YAG pumped dye laser in a rare-gas mixture (200 mbar Kr and 580 mbar Ar). The second step of the excitation is driven by a second frequency-doubled Nd:YAG pumped dye laser operating in the range 365–370 nm. The long path length of the gas beam and the short pulse width of the photolysis and excitation lasers (9 ns) allows characterization of the velocity distribution, by measuring the pulsed field-ionization signal as a function of time delay between photodissociation and H-atom excitation, and also allows a small velocity spread ($\sigma \sim 1\%$) to be selectively excited. An extractor mesh is mounted 1 cm from the surface so that a homogeneous field perpendicular to the surface can be applied 500 ns after Rydberg excitation. The field extracts ions that are formed by surface ionization (~ 4.5 $\mu$s later) and sends them a distance of 12 cm to the microchannel plate detector. The amplified output is integrated over an appropriate time gate to give the total surface-ionization signal [8,9]. In addition to the ion-extraction field, a variable constant homogeneous field can be applied at the time of excitation to generate the energy splittings enabling selection of Stark states. The applied Stark field also removes any ions in the interaction region before surface interaction. To detect surface ionization, the ion-extraction field must be sufficiently large to counteract the image-charge attraction of the ions and their incoming momenta towards the surface. Assuming a free-electron model for the surface image charge, the minimum ionization distance, $D_{\min}$, at which an ion can be turned around for a field, $E$, is given by

$$D_{\min}(E, T_\perp) = \frac{T_\perp + \sqrt{E} + \sqrt{T_\perp^2 + 2T_\perp\sqrt{F}}}{2E} \qquad (1)$$

(in atomic units), where $T_\perp = \frac{1}{2}mv_\perp^2$ is the kinetic energy of the ion perpendicular to the surface.

The UV and VUV laser polarizations are perpendicular to the field axis, populating mainly $m_l = 0, \pm 2$, and a small fraction of $m_l = \pm 1$ [22]. The *most extreme* red and blue states of the given $n$ manifold have pure $m_l = 0$ character. The inset of Fig. 1 shows the spectrum of the $n = 23$ Stark manifold populated in a homogeneous field and detected using pulsed-field ionization.

Figure 1 shows the surface-ionization profiles (surface-ionization signal *vs* extraction field) for selected $n = 23$ Stark states. As the field increases, the signal rises slowly and the low-field onset is determined by the minimum field required to extract the ions for the maximum ionization distance. The high-field cutoff is determined by the field ionization of the H atoms before they reach the surface and occurs progressively later on moving from the most

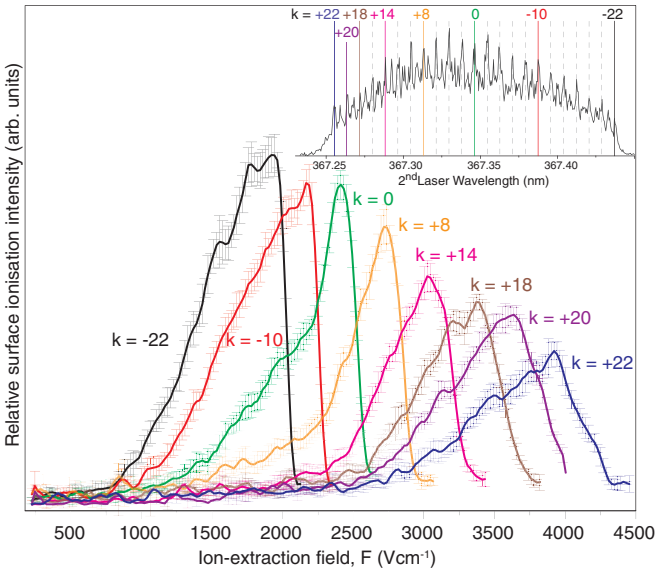


FIG. 1 (color online). Surface-ionization profiles for various $n = 23$ Stark states (marked by full lines in the inset). The Rydberg atoms have a mean collisional velocity of $\bar{v}_\perp = 650\ \mathrm{ms}^{-1}$ (with spread $\sigma_{v_\perp} \sim 5\ \mathrm{ms}^{-1}$). The intensities are corrected by the field-ionization signal shown by the inset. Inset: Field-ionization spectrum of $n = 23$ Stark states excited at $208 \pm 1\ \mathrm{V\,cm}^{-1}$. Dashed lines mark the calculated energies of $m_l = 0, \pm 2$ states.

redshifted states to the most blueshifted states, in keeping with the expected diabatic field ionization of the hydrogenic Stark states [19]. Similarly, the onset of the surface-ionization signal occurs progressively later from the most redshifted, surface-oriented states (which ionize furthest from the surface), to the most blueshifted, vacuum-oriented states (which ionize closest to the surface). As in the case of the field ionization, the ionization rate is lowest for the blueshifted state where the electron density is located furthest from the saddle point along the surface-atom normal. These results demonstrate that, unlike the case of Xe (and $H_2$), where the control of Stark polarization is lost at the surface due to level crossings between redshifted and blueshifted states from neighboring $n$ manifolds [13], it is possible to maintain the Stark polarization of H atoms from excitation to surface interaction. The system passes diabatically through any level crossings on approach to the surface.

Figure 1 also shows that the integrated surface-ionization signal is progressively smaller from the most redshifted state to the most blueshifted state. For Rydberg states that ionize very close to the surface, the field required to overcome the image-charge attraction and extract *all* the ions formed at the surface can be greater than the field-ionization threshold, and only a fraction of ions that ionize sufficiently far from the surface may be detected. Using Eq. (1) the surface-ionization distance can be estimated by assuming that the Rydberg atoms approach the metal surface at constant velocity. Figure 2 shows that for

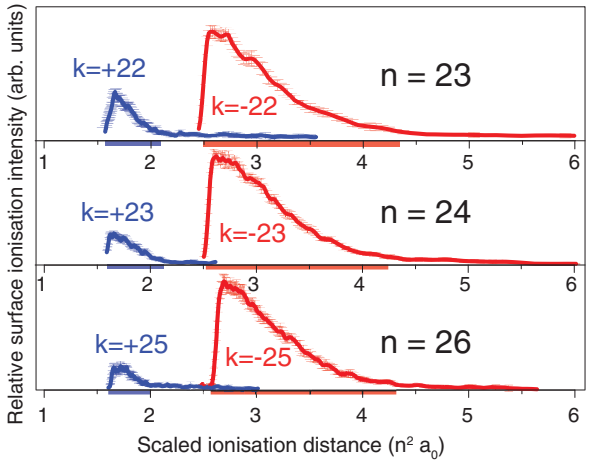


FIG. 2 (color online). Surface-ionization signal for the most extreme redshifted and blueshifted $m_l = 0$ states of the $n = 23$, 24, 26 manifolds plotted as a function of scaled ionization distance (by $n^2$), calculated from Eq. (1), assuming the Rydberg atoms approach the metal surface at a constant velocity of $v_\perp = 650\ \mathrm{ms}^{-1}$.

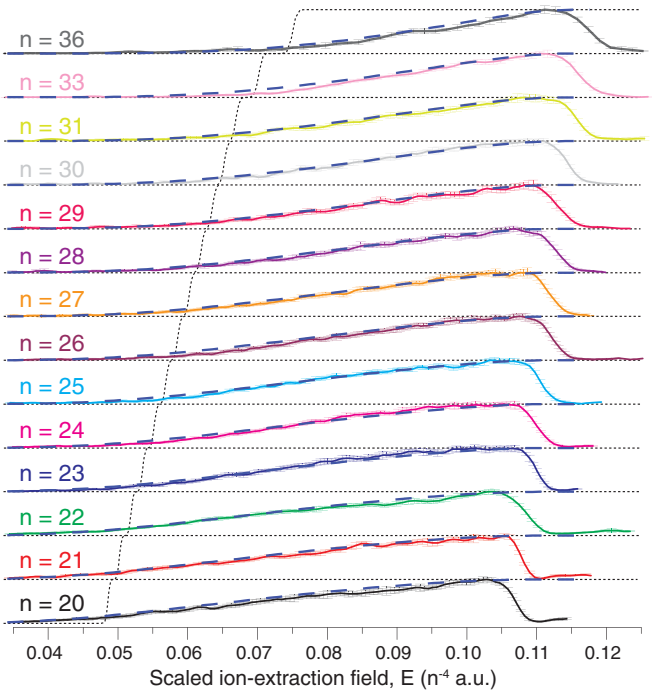


FIG. 3 (color online). Full lines: surface-ionization profiles for the most redshifted $k = (1 - n)$, $m_l = 0$ state of the $n = 20$–36 manifold. The Rydberg atoms have a mean collisional velocity of $\bar{v}_\perp = 650\ \mathrm{ms}^{-1}$. Dotted lines: results of OTB calculations. Dashed lines: results of the semiempirical model (see text).

the most redshifted Stark states of the $n = 23$, 24, 26 manifolds, surface ionization occurs at $(2.5\text{–}4.3)n^2a_0$, and at $(1.6\text{–}2.1)n^2a_0$ for the most blueshifted states, in line with theoretical predictions [10,12]. Note that the ion signal for the most blueshifted states of $n > 28$ manifolds is negligible, because the field required to extract the ions from the maximum ionization distance is beyond the field-ionization threshold.

As discussed above, it is of interest to compare quantitatively the experimental results with the theoretical predictions of this much-studied H-atom system. Here, we focus on the behavior of the most redshifted Stark states, for which the simple classical over-the-barrier (OTB) approach is approximately valid [20]. Briefly, the OTB approach involves the calculation of a critical distance $D_c(E)$ at which the surface-perturbed energy of the Rydberg state drops below the saddle point energy for a given external electric field, $E$. The Rydberg state energy near the surface is calculated by perturbation theory [23], and $D_c(E)$ is found numerically (and is $\sim \propto n^2$). Using Eq. (1), the ion-detection probability corresponding to the experimental surface-ionization profiles is given by the convolution of the velocity distribution of the Rydberg atoms with a step function at which $D_c(E) \geq D_{\mathrm{min}}(E, T_\perp)$.

Figure 3 shows the surface-ionization profiles for the most redshifted states of the $n = 20$–36 manifold (full lines) and the corresponding OTB predictions (dotted lines). The classical OTB approach provides a good estimate for the onset of ion signal, but does not account for the observed shallow rise in ion signal with field. The observed experimental profiles appear broader than the OTB prediction and shifted to higher average fields. The origin for the discrepancy with classical theory may arise from two effects. The first is the acceleration of the atom as it approaches the surface due to the dipole image-charge attraction. Quantum wave packet calculations with the inclusion of mean-field effects on the nuclear trajectory for $n = 10$ H atoms, have shown that acceleration of the Rydberg state towards the surface can be significant [12]. The effect is to shorten the ionization distance and decrease the detectability, shifting the surface-ionization profiles to higher fields. The second effect may be due to local surface patch fields, which have been shown by Dunning and coworkers to strongly affect the surface ionization of Rydberg Xe atoms [20], and can result in broad ionization profiles similar to those observed here.

The experimental results can be modeled very well by incorporating the effects of broadening and the shifting of the ionization distances empirically into the classical OTB approach: the mean critical surface-ionization distance is shifted $\mu(E) = D_c(E) - n^2$, and a spread of critical distances is introduced with a standard deviation $\sigma = 2.5n^2 a_0$. The cumulative ionization probability at distance $D$ from the surface is then given by a normal cumulative distribution function,

$$\Upsilon(D, E) = 1 - \frac{1}{2}\left[1 + \mathrm{erf}\left(\frac{D - \mu(E)}{\sqrt{2\sigma^2}}\right)\right]. \qquad (2)$$

The ion-detection probability at field $E$ is again given by the convolution with the velocity distribution of the Rydberg atoms $f(v_\perp)$:

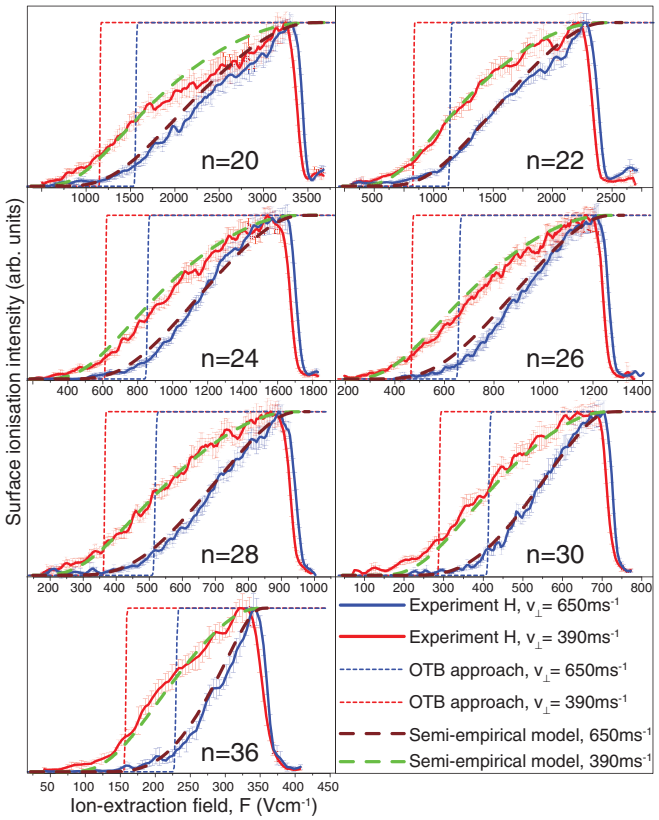


FIG. 4 (color online). Surface-ionization profiles of the most redshifted $m_l = 0$ states of the $n = 20$–36 manifolds for H atoms with a mean collisional velocity of $\bar{v}_\perp = 650$ ms$^{-1}$ and 390 ms$^{-1}$. The faster (slower) H atoms are selected from the gas packet of a pure $NH_3$ (20% $NH_3$/He) source.

$$S(E) = \int_0^\infty f(v_\perp)\Upsilon(D_{\min}, E)\mathrm{d}v_\perp, \qquad (3)$$

where $D_{\min}(E, T_\perp)$ is given by Eq. (1). The results are shown in Fig. 3 as dashed lines, and are in excellent agreement with the experimental results. A further test of the validity of the model given by Eq. (2), is shown in Fig. 4, which displays the ionization profiles of the most redshifted states of the $n = 20$–36 manifolds at two different mean collisional velocities. The collisional angle is kept constant at 15°, such that the Rydberg trajectory over the surface does not change, and the atoms of different velocities are selected by varying the gas mixture and time delay of the Rydberg excitation lasers. Changing the collisional velocity mainly affects the ion-detection probability [Eq. (1)], such that ions with lower perpendicular velocity are extracted more easily. Again, the OTB predictions (dotted lines) provide a good estimate of the onset of ion signal, and exhibit the same qualitative "shifts" as the experimental profiles for the different velocities, but do not account for the shallow rise in ion signal. The semi-empirical model (dashed lines) is again in very good agreement with the experimental profiles.

In conclusion, we have studied experimentally the surface-ionization dynamics of Rydberg hydrogen atoms, which provides a bridge between theory and experiment. By studying various Stark states which range from surface- to vacuum-oriented, the preservation of the polarization of the Rydberg states as they approach a surface and undergo ionization has been demonstrated. Unlike the nonhydrogenic case, it is possible to have genuine control over the orientation of the electron density distribution in the surface-ionization process. The extension of quantum calculations of surface-ionization rates to the range of principal quantum numbers employed here is challenging even for the H atom, and the current focus is on developing appropriate scaling relationships from wave packet calculations for lower $n$. Calculations incorporating patch-charge effects to try to understand fully the semiempirical modeling of the surface-ionization profiles will also be reported in future work.

The work presented here has concentrated on the properties of the Rydberg state, while the charge-transfer process is also dependent on the nature of the metal surface. The gold surface studied in this work is representative of a typical "free-electron" metal, where the Rydberg electron can be transferred to the metal conduction band unrestrictedly. One of the focuses of future experimental studies will be the effects of electronically structured metal surfaces (e.g., band-gap metal) on the charge-transfer process, where the incident Rydberg state can act as an energy resolved probe of the surface electronic states.

[1] M. P. Robinson *et al.*, Phys. Rev. Lett. **85**, 4466 (2000).
[2] N. Stolterfoht *et al.*, Scanning Microsc. **12**, 437 (1998).
[3] J. Mozley *et al.*, Eur. Phys. J. D **35**, 43 (2005).
[4] A. Tauschinsky *et al.*, Phys. Rev. A **81**, 063411 (2010).
[5] N. A. Nguyen, B. K. Dey, M. Shapiro, and P. Brumer, J. Phys. Chem. A **108**, 7878 (2004).
[6] J. Burgdörfer, P. Lerner, and F. Meyer, Phys. Rev. A **44**, 5674 (1991).
[7] D. F. Gray, Z. Zheng, K. A. Smith, and F. B. Dunning, Phys. Rev. A **38**, 1601 (1988).
[8] S. B. Hill *et al.*, Phys. Rev. Lett. **85**, 5444 (2000).
[9] G. R. Lloyd, S. R. Procter, and T. P. Softley, Phys. Rev. Lett. **95**, 133202 (2005).
[10] J. Hanssen, C. F. Martin, and P. Nordlander, Surf. Sci. **423**, L271 (1999).
[11] N. N. Nedeljković and D. K. Božanić , Phys. Rev. A **81**, 032902 (2010).
[12] E. So, M. T. Bell, and T. P. Softley, Phys. Rev. A **79**, 012901 (2009).
[13] F. B. Dunning, H. R. Dunham, C. Oubre, and P. Nordlander, Nucl. Instrum. Methods Phys. Res., Sect. B **203**, 69 (2003).
[14] E. A. McCormack, M. S. Ford, and T. P. Softley, J. Phys. Chem. A **114**, 11 175 (2010).
[15] J. Sjakste, A. G. Borisov, and J. P. Gauyacq, Phys. Rev. A **73**, 042903 (2006).

[16] N. S. Simonovic and J. P. Salas, Phys. Lett. A **279**, 379 (2001).
[17] K. Ganesan and K. T. Taylor, J. Phys. B **29**, 1293 (1996).
[18] A. Borisov, D. Teillet-Billy, and J. Gauyacq, Nucl. Instrum. Methods Phys. Res., Sect. B **78**, 49 (1993).
[19] T. F. Gallagher, *Rydberg Atoms* (Cambridge University Press, Cambridge, England, 1994).
[20] Y. Pu, D. D. Neufeld, and F. B. Dunning, Phys. Rev. A **81**, 042904 (2010).
[21] S. Willitsch, J. M. Dyke, and F. Merkt, Helv. Chim. Acta **86**, 1152 (2003).
[22] C. Delsart, L. Cabaret, C. Blondel, and R. J. Champeau, J. Phys. B **20**, 4699 (1987).
[23] A. Borisov, R. Zimny, D. Teillet-Billy, and J. Gauyacq, Phys. Rev. A **53**, 2457 (1996).